

Melt-textured $\text{Bi}_{1.6}\text{Pb}_{0.4}\text{Sr}_2\text{Ca}_2\text{Cu}_3\text{O}_{11}$ bulk superconductors fabricated in a simple tube furnace

Z. L. DU, Z. H. HE

Physics Department, Zhongshan University, Guangzhou, China

P. C. W. FUNG, J. C. L. CHOW, T. F. YU

Physics Department, The University of Hong Kong, Hong Kong

Using the simplified version of the melt-textured growth (MTG) technology with a simple tube furnace, we have fabricated superconductors satisfying the nominal composition $\text{Bi}_{1.6}\text{Pb}_{0.4}\text{Sr}_2\text{Ca}_2\text{Cu}_3\text{O}_{11}$. We would note that the material used in the fabrication was prepared by mixing a precursor $\text{Bi}_{1.6}\text{Pb}_{0.4}\text{Sr}_2\text{Cu}_3\text{O}_x$ and CaO powder. This two step technique was found to be superior to the single step solid state reaction method after many trials. Scanning electron microscopy (SEM) and transmission electron microscopy (TEM) morphologies show that the melt-textured bulk samples are made up of stacks of highly textured single crystal-like layers. X-ray analysis as well as d.c. magnetization measurements were carried out and the J_c value was found to be $1.3 \times 10^3 \text{ A cm}^{-2}$ at 77 K using the Bean model. At this stage, though J_c is not so high as that of the best samples obtained from other complicated methods involving special (hot) pressing and sintering techniques, we do not need to apply any mechanical treatment at or after the heating procedure.

1. Introduction

During the last two years, much effort has been focused on increasing the critical current densities of ceramic superconducting bulk samples. One general line of thought is to minimize the number of weak links in the sample. The most effective way perhaps is to fabricate samples with highly textured crystal alignments. The melt-textured growth (MTG) process was developed [1–7] for the $\text{YBa}_2\text{Cu}_3\text{O}_{7-y}$ (YBCO) specimen – the sample materials (inside a porcelain cup) had to be moved slowly and steadily inside the furnace while the heating process was conducted [2, 3]. Then the modified version of the MTG process was introduced in programmable three-zone furnace in order that non-zero gradients of temperature existed in the heating chamber and the sample was fixed in space [8]. Varying the temperatures over spatial points in time, the heat treatment received by the stationary sample is equivalent to that received by the “travelling cup” stated. This modified MTG method was further simplified by putting the samples near both ends of a common tube furnace [9–10] and operating the heating programme in special steps each of which serves a particular purpose [11]. For example, in step (ii) of [12], the material was purposely heated to a temperature $> 1050^\circ\text{C}$ so that apart from a compound Y_2BaCuO_5 , other materials were melted. The Y-211 particles were speculated to be the nuclei of crystal growth as the temperature was lowered. In fact, it is believed that the success of the MTG for the

YBCO class of samples was realized much readily on the physical existence of crystal growth nuclei in the melt state [9]. The resulting samples have highly oriented crystal layers even up to the mm scale.

The second origin of J_c enhancement is believed to arise from the existence of magnetic flux pinning centres in the bulk samples. For some time it was believed [10–18] that the Y-211 particles of approximately a few μm in size were the pinning centres. Recent microstructure analyses [19] seem to indicate that the pinning centres might be much smaller in spatial scale. For example, it has been demonstrated [12] that the appearance of microdefects with sizes ~ 1 to several nm are associated with samples with relatively high J_c values whereas the J_c values of samples showing higher degree of crystal structure regularity were relatively low. Moreover particles with sizes of approximately a few tens of nm were found to be associated with regions with high atomic ratio of Y:Ba:Cu = 2:1:1 [13]. Though one cannot conclude that such microdefects are the only origins of flux pinning and are therefore the causes of J_c enhancement, the relation between the abundance, size of Y_2BaCuO_5 grains and J_c would be a very interesting property yet to be investigated.

On the other hand, much effort has been spent on fabricating (BSCCO) samples with crystal texture structure also. Repeated sintering and pressing has been applied to arrive at samples with flake-like crystals which are larger in area than the common

polycrystalline grains [20]. The established powder-in-tube technique [21–23] for the BSCCO class led to J_c values approximately several 10^3 A cm^{-2} . An elaborate optimum sintering procedure with the help of differential thermal analyser was introduced to make an almost pure 2223 phase Bi-specimen [24]. A rather complicated mechanical deformation pressing technique was used to fabricate BSCCO/Ag microcomposite ribbons with c-axis oriented texture and the J_c value was found to have been enhanced, reaching $6 \times 10^3 \text{ A cm}^{-2}$ [25]. The sophisticated melt-textured growth method in [26] led to samples with J_c up to about 1000 A cm^{-2} at 68 K. In [27], the Pb doped Bi-specimens were hot-pressed under a uniaxial compression at 822°C and J_c was increased to $7 \times 10^3 \text{ A cm}^{-2}$ at 77 K and under 10 gauss. Thick superconducting BSCCO films were prepared under a constant stress at 855°C and the J_c reached was reported to be up to $9.5 \times 10^3 \text{ A cm}^{-2}$ [28]. Again, sintered pellets were deformed mechanically by a constant displacement rate in the temperature range of $830\text{--}860^\circ\text{C}$ and flake-like crystals were observed under scanning electron microscopy (SEM) with a flake size $\sim 30 \times 30 \mu\text{m}^2$ [29]. The low J_c ($< 200 \text{ A cm}^{-2}$) was attributed to formation of non-superconducting phases between the flakes. Other sophisticated fabrication techniques have been developed recently by researchers in this area. For example, 2223 tapes sheathed under Ag were processed with fine aerosol spray pyrolysis powder and the phase formation at the Ag-ceramic interface was studied [30]. Further development in the sinter forging process has just been developed [31] to form bulk samples with strong textures in which the c-axes of the flakes were aligned preferentially along the direction of pressing; the flakes appeared to form continuous thin wavy layers after the pressing treatment. In all these, plus other studies, certain mechanical treatments were applied to the sample materials during sintering or between sintering processes. It would be fruitful also to work from another direction; developing method(s) to fabricate bulk samples with texture and high critical current density (compared to that of the common polycrystalline samples) using only thermal treatment. This investigation serves to report the result of such a method and we shall show here that bulk samples with good crystal texture can be fabricated using special thermal treatment alone. Our attempt at this stage is to develop a simple MTG process for the BSCCO class, in parallel to that of the YBCO family.

2. Experimental procedure

It is well-known that it is difficult to fabricate the pure 2223 phase of the bismuth family without doping(s) [32–36]. Pb is known to be a nominal dopant. We first observe that out of the oxides of Bi, Pb, Sr, Ca and Cu, CaO has the highest melting point of 2614°C . Though CaO might react with other elements during heating, there is the possibility that, since the formation of 2223 or 2212 phases takes a long sintering time, some CaO (and perhaps other Ca compound) would be left as solid particles while other materials are in the

melt state during a short time period of 10 min at 950°C . We thus purposely employed the two-step approach in making our samples and hoped that sufficient crystal nuclei were left to help crystal growth.

In our procedure, we ground powders of Bi_2O_3 , PbO , SrCO_3 and CuO to a mixture with particle size $\sim 1 \mu\text{m}$ and heated the materials at 750°C for 40 h according to the nominal composition of $\text{Bi}_{1.6}\text{Pb}_{0.4}\text{Sr}_2\text{Cu}_3\text{O}_9$. The resulting material was found to be partially crystallized. Two moles of CaO was added to one mole of $\text{Bi}_{1.6}\text{Pb}_{0.4}\text{Sr}_2\text{Cu}_3\text{O}_9$ and the mixture was pressed into a pellet of size $\approx 11 \times 5 \times 1 \text{ mm}^3$. The pellet was placed near one end of our tube furnace (Linberg 847) where the temperature gradient at 950°C was $\sim 10^\circ\text{C cm}^{-1}$. We carried out this melt-textured process according to the thermal treatment of Fig. 1. We repeated such treatment for two samples. Sample A was quenched in air after reaching 870°C and sample B was heated at 870°C for a further time interval of 50 h in O_2 and then quenched in air. A reference sample, i.e. sample C was sintered in a muffle furnace at 860°C for 100 h.

The resistance– T curves for these three samples are shown in Fig. 2(a). Clearly, sample C contains much more 2212 phase and sample B is obviously the best sample here. The real part of the a.c. susceptibilities for both samples is presented in Fig. 2(b). Note that though the amount of 2223 phase is relatively small in each case, the microstructure of these two samples are significantly different from that of the normal polycrystalline samples. X-ray diffraction analysis was performed on sample B with a D/mak diffractometer using $\text{CuK}\alpha$ radiation and Fig. 3 shows the result. The peaks corresponding to the 2212 phase are indicated by * while those for the 2223 phase are indicated by small circles. Crystal parameters of a , b and c found for the 2212 phase are $a = b = 0.34 \text{ nm}$, $c = 3.09 \text{ nm}$ whereas those found for the 2223 phase are $a = b = 0.38 \text{ nm}$, $c = 3.71 \text{ nm}$. The microstructure of these two samples are significantly different from that of the normal polycrystalline samples. Fig. 4(a–c) shows SEM morphology (SEM model: Cambridge Stereoscan S150) of sample A, B and C in the $5 \mu\text{m}$ length scale. A similar set of three

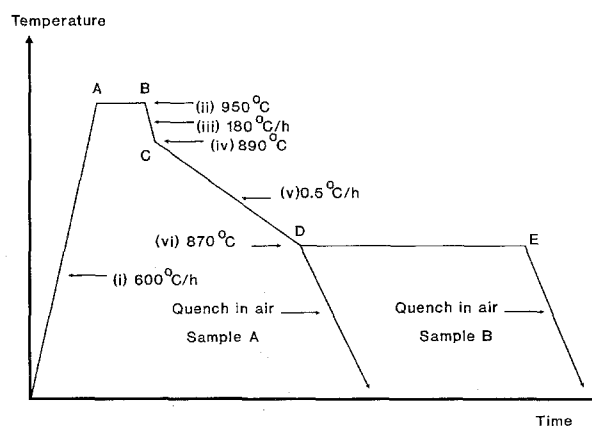


Figure 1 Heat treatment profile for the melt-textured process. AB = 20 min; DE = 40 h.

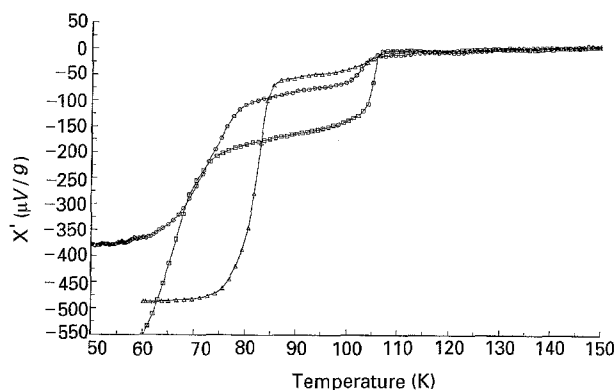
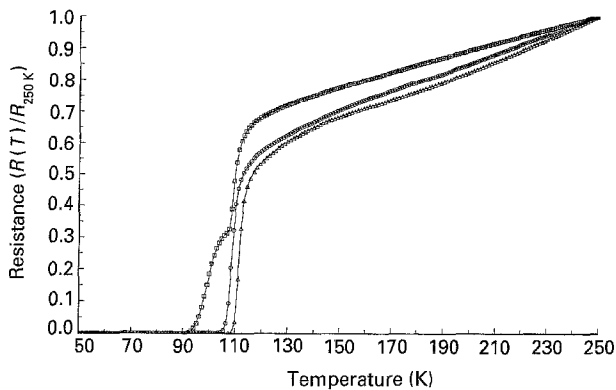


Figure 2 (a) R - T relation for the samples A, B and C. \circ , A; \triangle , B; \square , C; $I = 10$ mA. (b) Real part of the a.c. susceptibilities for samples A, B and C. \circ , A; \triangle , B; \square , C; $I_{ac,pp} = 20$ mA, $F = 120$ Hz.

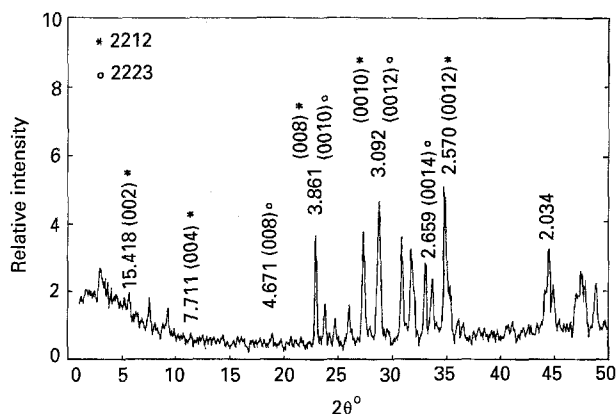


Figure 3 X-ray diffraction pattern for sample B. \bullet , 2212; \circ , 2223.

micrographs with a $50 \mu\text{m}$ (Fig. 4(d, e)) and $25 \mu\text{m}$ (Fig. 4(f)) scale are shown for the purpose of comparison. Moreover, energy dispersive spectroscopy (EDX) analysis (model: Link-eXL) was carried out in sample B. In each case, the pellet was first broken into two pieces so as to obtain a freshly fractured surface. Ten points were then selected on a single crystal layer. The atomic percentages of Bi, Sr, Ca, Cu and Pb detected from EDX are displayed in Table I, as a typical example. It was found that the specimen contained a number of phases and Pb exists inside the layer. This shows that Pb is in fact substituting into the crystal layer, and the sample is a mixed-phase one.

A small part of each sample was ground into a powder of size $\sim 1 \mu\text{m}$ in absolute alcohol. The choroid material was cast into a conical-like embedding plastic mould. Epoxy resin (tabb 812) was filled into the mould covering the sample material. The mould was then dried in an oven for 14 h at 60°C . Having trimmed the cross-sectional area of the resin tip containing the Bi-Sr-Ca-Cu-O powder, the resin was inserted into a commercial sectioning machine (model Ultra Cut) for cutting. A diamond knife with cutting angle of 45° was employed to section the sample materials, producing films of thickness ≈ 70 - 80 nm. These films were left floating on water surface and aluminium grid with formvar was used to carry them away for TEM observation (TEM model: Jeol JEM 2000 FX), after drying in air and the usual carbon coating procedure.

Fig. 5 shows a typical TEM micrograph of the melt-textured Bi-family sample B. Parallel crystal lattice fringes with spacing ≈ 1.6 nm are clearly shown in Fig. 5. Note that the spacing measures $1/2$ the c -axis [37] and thus the full c -axis cast an image of 3.2 nm on the micrograph. Finally, d.c. magnetization measurement was carried out for sample B and the M-H loop was obtained in the manner reported in ref. [9] (Fig. 6). Compared to that of the YBCO sample, the area is relatively small. However, the J_c value deduced using the equation of [38], with reference to the Bean model, was found to be $1.3 \times 10^3 \text{ A cm}^{-2}$, being significantly larger than that of the polycrystalline samples, typically ~ 1 to about 100 A cm^{-2} .

3. Discussion

(1) Since calcium oxide has a higher melting temperature than any of the Bi, Pb, Sr and Cu oxides, we have prepared the precursor first without CaO according to the nominal composition as stated. CaO was then added in before different stages of sintering as depicted in Fig. 1. In fact more than 40 heating programmes were tried in the present work using stoichiometric ratios $\text{Bi}_{2-x}\text{Pb}_x\text{Sr}_2\text{Ca}_2\text{Cu}_3\text{O}_{11}$ ($x = 0 \dots 0.6$) without precursors and the SEM morphologies of these samples were not much different from those prepared by the non-MTG methods. Fig. 4(b) for example, of this investigation (plus many others we have taken) indicates clearly that very thin crystal layers (of thickness $\sim 0.5 \mu\text{m}$) were formed and these layers tightly stacked up in many parts of the sample. Though empty space occurs between stacks of flakes of superconducting materials, we have fabricated bulk samples with good texture and typical flake which have an area $\sim 40 \times 40 \mu\text{m}^2$, and the thickness of a good stack of flakes is about $20 \mu\text{m}$.

(2) Though the R - T curves indicate that T_c ($R = 0$) is 108 and 109 K for samples A and B respectively, the real part of the a.c. susceptibilities, X-ray diffraction analysis as well as EDX data show that clearly two phases co-exist; these phases are obviously the 2212 and 2223 phases. The 2223 phase exists in a relatively small amount, and it is believed that improvement of this melt-textured method would lead to enhancement of the high temperature phase. The imaginary part χ'' with

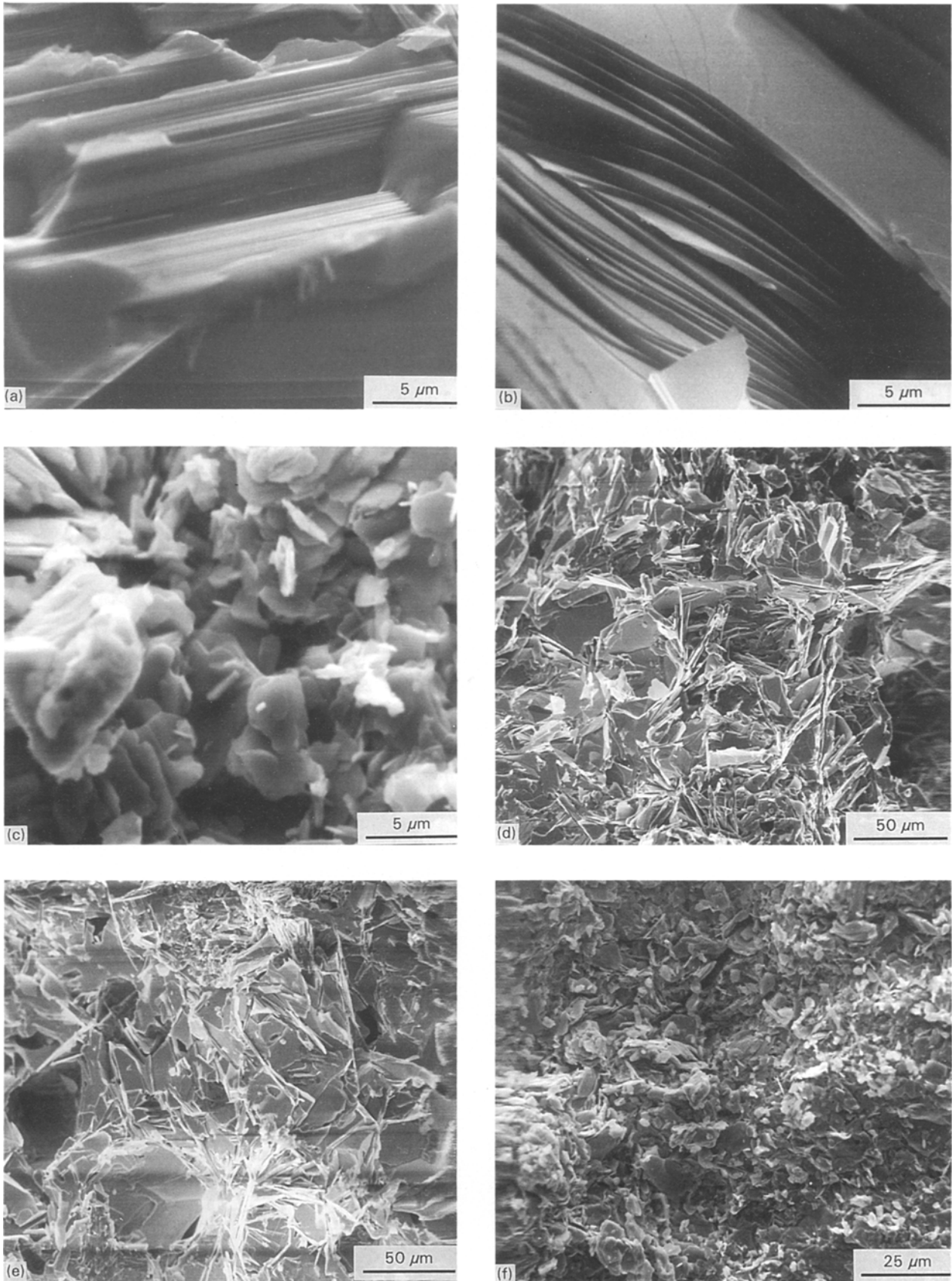


Figure 4 (a) SEM morphology of sample A with a scale of 5 μm . (b) SEM morphology of sample B with a scale of 5 μm . (c) SEM morphology of sample C with a scale of 5 μm . (d) SEM morphology of sample A with a scale of 50 μm . (e) SEM morphology of sample B with a scale of 50 μm . (f) SEM morphology of sample C with a scale of 25 μm .

respect to change in frequency, external magnetic field etc. should be carried out before it will be possible to provide useful information about the flux-pinning mechanism involved in this class of melt-textured specimens.

(3) The TEM morphology analysis reported here reveals that lattice fringe lines of spacings $\approx 1.6 \text{ nm}$ appear and these fringes stretch throughout a significant portion of the TEM sample. Obviously such a result

TABLE I Atomic percentages of Bi, Sr, Ca, Cu and Pb of the 10 selected points in a single crystal-like layer of sample B

Spot number	Atomic % of Bi	Atomic % of Sr	Atomic % of Ca	Atomic % of Cu	Atomic % of Pb
1	14.65	5.70	8.17	18.07	1.69
2	14.38	5.54	7.94	18.55	1.92
3	14.32	5.42	8.20	18.16	1.93
4	14.04	5.28	8.12	18.72	2.01
5	14.10	5.05	8.21	18.94	1.80
6	14.08	5.00	8.15	18.84	2.05
7	13.91	4.84	8.13	19.55	1.78
8	10.53	3.95	13.91	13.92	5.43
9	12.18	4.41	11.00	16.56	3.75
10	13.37	4.75	8.17	19.62	1.98

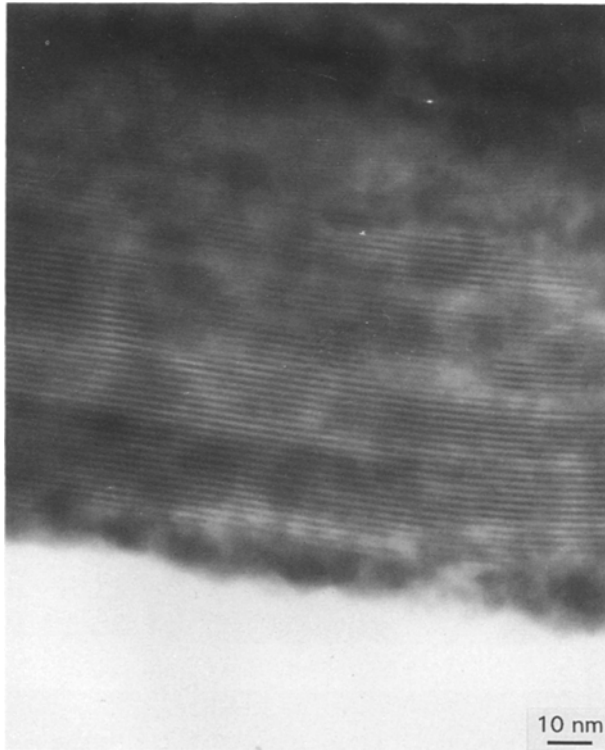


Figure 5 TEM morphology of sample B.

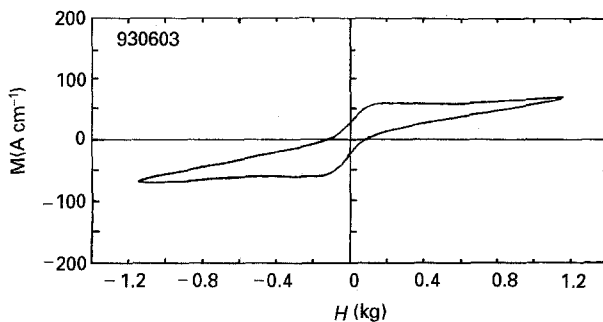


Figure 6 D.c. magnetization hysteresis loop for sample B.

together with the X-ray diffraction analysis suggests that the 2212 and 2223 phases coexist, in line with the macroscopic susceptibility measurement.

(4) The degree of difficulty in fabricating the melt-textured Bi-family members is higher than that of the Y-family members, as experienced by our research group and others. Since the Bi-members are in general

more stable than the Y-123, Y-145 [39] specimens, successful fabrication of melt-textured and hence MTG Bi-family superconductors has an important bearing in future application of ceramic superconductors.

(5) D.c. magnetization measurement indicates that the melt-textured samples, with B as an example, have J_c values greater than 1000 A cm^{-2} . Certainly this is smaller than that obtainable using more complicated processes involving mechanical pressing as stated in Section 1. If, however, we can improve further the qualities of the melt-textured samples, or if we use such melt-textured sample materials as the starting point of the tape or wire making processes, very high J_c values would be anticipated.

Acknowledgements

Z.L. Du is Visiting Scientist to the University of Hong Kong under the Visitorship of Academic Staff from Universities in China to visit the University of Hong Kong programme. Part of the work of Z.L. Du was supported by the Specific Foundation of National Education Committee for Doctor Station in Advanced University.

T.F. Yu and J.C.L. Chow are Ph.D candidates of the University of Hong Kong.

The authors thank Mr. Y.C. Mok and A.S.L. Wong for their helpful assistance in the TEM sample preparation starting with melt-textured powders.

References

1. M. MURAKAMI, *Supercond. Sci. Technol.* **5** (1992) 185.
2. G. G. KACHARAVA, YU F. EI'TSEV, V. R. KARASIK, E. YU DOVIDENKO and G. A. TSINTSADZE, *ibid.*, **4** (1991) 707.
3. K. SALAMA and V. SELVAMANICKAM, *ibid.*, **5** (1992) S85.
4. N. OGAWA, M. YOSHIDA, I. HIRABAYASHI and S. TANAKA, *ibid.*, **5** (1992) S89.
5. M. R. LEES, P. DE. RANGO, D. BOURGAULT, J. M. BARBUT, D. BRAITHWAITE, P. LEJAY, A. SULPICE and R. TOURNIER, *ibid.*, **5** (1992) 362.
6. REN HONGTAO, HE QING, XIAO LING, WANG RUIKUN and YU DINGAN, *Cryogenics* **30** (1990) 837.
7. T. LEVENTOURI and F. D. MEDINA, *Solid State Communications* **85** (1993) 675.
8. I. MONOT, M. LEPROPRE, J. PROVOST, G. DESGARDIN, B. RAVEAU, D. BOURGAULT, J. M. BARBUT, D. BRALTHWAITE and R. TOURNLER, *Supercond. Sci. Technol.* **5** (1992) 712.

9. Z. L. DU, P. C. W. FUNG, Z. H. HE, G. H. ZHOU, M. J. LI, Y. LU and J. X. ZHANG, *J. Superconductivity* **6** (1993) 27.
10. P. C. W. FUNG, Z. L. DU, J. C. L. CHOW, Z. H. HE, T. F. YU, Y. Y. LUO, Q. Y. LI and Y. LU, *Physica C* **212** (1993) 279.
11. P. C. W. FUNG, J. C. L. CHOW, T. F. YU and Z. L. DU, *J. Superconductivity*, **6** (1993) 247.
12. Z. L. DU, P. C. W. FUNG, J. C. L. CHOW, T. F. YU, Z. H. HE, Y. LI, Y. Y. LUO and J. X. ZHANG, *Physica C*, **215** (1993) 319.
13. FENG YOUNG, ZHOU LIAN, ZHANG PINGXIANG, WANG KEGUANG, JI PING, WU XIAOZU, LUO CHANGXUN and XING MIANRONG, *Supercond. Sci. Technol.* **5** (1992) 432.
14. P. A. GODELAINE, C. HANNAY, R. CLOOTS, H. W. VANDERSCHUREREN, G. J. TATLOCK, D. G. MCCARTNEY and M. AUSLOOS, *ibid.*, **4** (1991) 701.
15. H. FUJIMOTO, M. MURAKAMI, S. GOTOH, K. YAMAGUCHI, M. YOSHIDA, T. TAKATA, N. KOSHIZUKA and S. TANAKA, *ibid.*, **5** (1992) S93.
16. P. KOTTMAN, H. JONES, A. J. FRPST and C. R. M. GROVENOR, *ibid.*, **5** (1992) 381.
17. CHANG-GENG CUI, FENG-SHENG LIU, HUI-LIN MOU, TIAN-CHEN WANG, SHAN-LIN LI, JUN LI, LIU HONGYUEM LIAN ZHOU and XIAO-ZU WU, *Cryogenics* **30** (1990) 603.
18. S. T. DING, J. W. LIN, X. JIN, ZHENG YU, X. X. YAO, H. L. MOU and L. ZHOU, *ibid.*, **5** (1992) S240.
19. FENG YOUNG and ZHOU LIAN, *Physica C* **202** (1992) 298.
20. S. X. DOU, H. K. LIU, J. WANG and W. M. BIAN, *ibid.*, **4** (1991) 21.
21. K. SATO, T. HIKATA, H. MUKAI, M. UHEYAMA, N. SHIBUTA, T. KATO, T. MASUDA, M. NAGATA, K. IWATA and T. MITSUI, *IEEE Trans. Magn.* **27** (1991) 1231.
22. K. CHEN, L. HORNG, H. S. KOO, C. Y. SHEI, L. P. WANG, C. CHIANG, T. J. YANG, W. H. LEE and P. T. WU, *Appl. Phys. Lett.* **59** (1991) 1635.
23. R. H. ARENDT, M. F. GARBAUSKAS, K. W. LAY and J. E. TKACZYK, *Physica C* **194** (1992) 383.
24. T. MATSUSHITA, A. SUZUKI, K. TERAMOTO, M. OKUDA and H. NATITO, *ibid.*, **4** (1991) 721.
25. WEI GAO and J. B. V. SANDE, *ibid.*, **5** (1992) 318.
26. O. KOTTMAN, HONES, A. J. FROST and C. R. M. GROVENOR, *ibid.*, **5** (1992) 381.
27. R. YOSHIKAWA, H. IKEDA, K. YOSHIKAWA and N. TOMITA, *Japan. J. Appl. Phys.* **29** (1990) L753.
28. N. MURAYAMA, Y. KODAMA, S. SAKAGUCHI and F. WAKAI, *J. Mater. Res.* **6** (1991) 1425.
29. XIAOMING YANG and T. K. CHAKI, *Supercond. Sci. Technol.* **6** (1993) 269.
30. YI FENG, Y. E. HIGH, D. C. LARBALESTIER, Y. S. SUNG and E. E. HELLSTROM, *Appl. Phys. Lett.* **62** (1993) 1553.
31. K. C. GORETTA, M. E. LOMMANS, L. J. MARTIN, J. JOO, R. B. PEOPPEL and NAN CHEN, *ibid.*, **6** (1993) 282.
32. T. MATSUSHITA, A. SUZUKI, K. TERAMOTO, M. OKUDA and H. NAITO, *ibid.*, **4** (1991) 721.
33. QING-RONG FENG, HAN ZHANG, SUN-QI FENG, XING ZHU, KE WU, ZUN-XIAO LIU and LI-XIN XUE, *Solid State Communications*, **78** (1991) 609.
34. S. C. BHARGAVA, J. S. CHAKRABARTY and TAJNI SHARMA, *Solid State Communications*, **78** (1991) 397.
35. MING XU, J. POLONKA, A. I. GOLDMAN and K. K. FINNEMORE, *Applied Superconductivity* **1** (1993) 53.
36. YING XIN, Z. Z. SHENG, F. T. CHAN, P. C. W. FUNG and K. W. WONG, *Solid State Comm.* **76** (1990) 1347, 1351.
37. CHEN XIANHUI, XU CHENG, CHEN ZUYAO, QIAN YITAI, CHEN ZHAOJIA, CAO LIEZHAO, *Supercond. Sci. Technol.* **6** (1993) 276.
38. SARMA, "Type-II Superconductivity" Chapter 9 (Pergamon Press, Oxford, 1989).
39. C. C. LAM, S. T. TANG, T. W. LI, C. L. FU, W. G. ZENG, P. C. W. FUNG, Z. M. LIU and W. Y. KWOK, *J. Phys. Chem. Solids*, **53** (1992) 499.

Received 13 October 1993
and accepted 27 July 1994